

# Indentation-induced deformation in the Serbian Carpathians: a structural and kinematic study in the TMC basin and the Lower Getic Unit

NIKOLA RANĐELOVIĆ<sup>1</sup> , MAJA MALEŠ<sup>1</sup> , MARIJA GRUJOVSKI  
STANISAVLJEVIĆ<sup>1</sup> , MARINKO TOLJIĆ<sup>1</sup> , BRANISLAV TRIVIĆ<sup>1</sup>   
& UROŠ STOJADINOVIC<sup>1</sup> 

## Key words:

*Indentation, Strain partitioning, Serbian Carpathians, TMC basin, Getic Unit.*

**Abstract.** A field structural study was performed in the Late Cretaceous Timok Magmatic Complex (TMC) basin and the underlying Lower Getic unit to improve understanding of post-Eocene tectonic evolution of the Serbian Carpathians. Our study demonstrates that Oligocene – Middle Miocene deformation is recorded in the TMC Basin, and it is characterized by strain partitioning between normal faults accommodating N–S to NW–SE extension and two distinct groups of strike-slip faults. In the central parts of the TMC basin, these structures controlled the opening of several Miocene intra-montane pull-apart basins. Southwards, the fault system change to a right lateral fault with a horse-tail geometry. Our observations indicate that Oligocene – Middle Miocene structures from the TMC and neighbouring units are an integral part of the previously defined Circum-Moesian Fault System that accommodated along-strike changes in the collisional mechanics of the Carpathians.

**Апстракт.** Теренска истраживања су извршена у горњокредном басену Тимочког магматског комплекса и структурно нижој јединици Доњег Гетикума, како би се унапредило разумевање постеоценске тектонске еволуције у Српским Карпатима. Наша студија показује да је олигоценско–средњомиоценска деформација захватила и ТМК басен. Одликује се значајном расподелом стреса између гравитационих раседа који су акomodирали С–Ј до СЗ–ЈИ правац екстензије и две различите групе транскурентних раседа. У централним деловима басена, наведене структуре су контролисале отварање више миоценских унутарпланинских басена. Насупрот томе, у јужним деловима, те структуре представљају део регионалног десног транскурентног раседа који показује „horse-tail“ геометрију. Наше опсервације указују да су олигоценско–средњомиоценске структуре развијене у ТМК басену и суседним јединицама саставни део раније дефинисаног Циркум-Мезијског раседног система који је акomodирао промене у механизмима колизије дуж пружања Карпатског орогена.

## Кључне речи:

*Индентација, Расподела стреса, Српски Карпати, ТМК басен, Гетска јединица*

<sup>1</sup>University of Belgrade, Faculty of Mining and Geology, Djušina 7, 11000 Belgrade, Serbia; E-mail: nikola.randjelovic@rgf.bg.ac.rs

## Introduction

The Serbian Carpathians, situated in a back-arc position of the Carpathian Orocline (Fig. 1a), preserve a record of complex poly-phase tectonic evolution. After the Middle Jurassic – Late Cretaceous closure of the Ceahlău-Severin branch of the Alpine Neotethys combined with the influence of the neighboring Neotethyan slab, the Serbian Carpathians were affected by intense collisional processes (CSONTOS & VÖRÖS, 2004; HORVÁTH et al., 2015; MATENCO, 2017; SCHMID et al., 2008, 2020). The latter is primarily marked by the indentation around the Moesian Platform and its interplay with coeval retreating subduction in the Eastern Carpathians (SÂNDULESCU, 1988; CSONTOS & VÖRÖS, 2004; USTASZEWSKI et al., 2008). Previous studies have determined that such mechanics during the Late Oligocene – Middle Miocene induced large-scale translations and rotations (RATSCHBACHER et al., 1993; VAN HINSBERGEN et al., 2020; MÁRTON et al., 2024), which was on a crustal-scale accommodated by significant strain partitioning (KRSTEKANIĆ et al., 2020, 2021, 2022). However, the structural pattern of the Late Oligocene – Middle Miocene deformation is still not defined for some parts of the orogen. In order to enhance the understanding of previously defined indentation mechanisms in the Serbian Carpathians, we conducted a field structural and kinematic study in the Late Cretaceous TMC basin and along its margins, made up by the Lower Getic unit.

## Orogenic structure of the Serbian Carpathians

The Serbian Carpathians are part of the broader Alpine–Carpathian–Dinarides orogenic system in southeastern Europe (Fig. 1a). The evolution of this complex orogen resulted from the geodynamic history of two neighbouring oceanic domains, the Alpine Tethys and the Neotethys, which separated various continental units during the Mesozoic (SCHMID et al., 2008; MATENCO et al., 2016). The transitional zone between the Dinarides and Carpathians in Serbia (Fig. 1b) represents a key position within the interference zone of two closely spaced oceanic branches that be-

long to the Neotethys and Alpine Tethys Oceans (i.e., the Vardar Ocean and the Ceahlău-Severin Ocean). The Vardar Ocean exhibits a northern branch of the Neotethys that opened during the Middle Triassic continental rifting, separating the western margin of the Europe-derived Dacia mega-unit from the Adria-derived Internal Dinarides (SCHMID et al., 2008, 2020). On the other side, the Middle Jurassic opening of the easternmost branch of the Alpine Tethys – the Ceahlău-Severin Ocean divided the eastern margin of Dacia and the Danubian Unit, which originated from the Moesian foreland (CSONTOS & VÖRÖS, 2004; HORVÁTH et al., 2015; MATENCO, 2017).

The Serbian segment of the double-curved Carpathian Orogen is located in its backarc-convex part (Fig. 1a) between the South Carpathians to the north, the stable Moesian Platform to the east, the Balkanides to the south, and the Dinarides to the west (Fig. 1b). In present-day geometry, it is exposed as a system of E-vergent nappe stack made up of tectonic units of European continental affinity (SCHMID et al., 2008, 2020; Fig. 1c). From west to east, these are represented by the Serbo-Macedonian Unit, the Supragetic Unit, and the Getic Unit, which together form parts of the Dacia Mega-Unit, the Ceahlău-Severin Unit, and the easternmost Danubian Unit (Figs. 1b,c).

The Serbo-Macedonian Unit (SMU) marks the westernmost segment of the Dacia Mega-Unit at its transition towards the Adria-derived units. It consists of medium-grade metamorphic rocks (DIMITRIJEVIĆ, 1997; ANTIĆ et al., 2016 a,b) exhumed during the Late Cretaceous extension along the E-dipping Morava ductile shear zone, located at the contact with the Supragetic Unit (STOJADINOVIC et al., 2021, 2024). On its western margin, the SMU is bounded by a system of brittle top-WSW thrusts marking its contact with the Internal Dinarides (MALEŠ et al., 2023). This thrusting occurred during the latest Cretaceous – Paleogene as a result of the final closure of the Vardar Ocean and the collision between the Adria- and Europe-derived continental units along the Sava suture zone (PAMIĆ, 2002; SCHMID et al., 2008; USTASZEWSKI et al., 2009, 2010; TOLJIĆ et al., 2018; STOJADINOVIC et al., 2022).

The next structurally higher Supragetic and Getic units consist of a Paleozoic greenschist- to amphi-

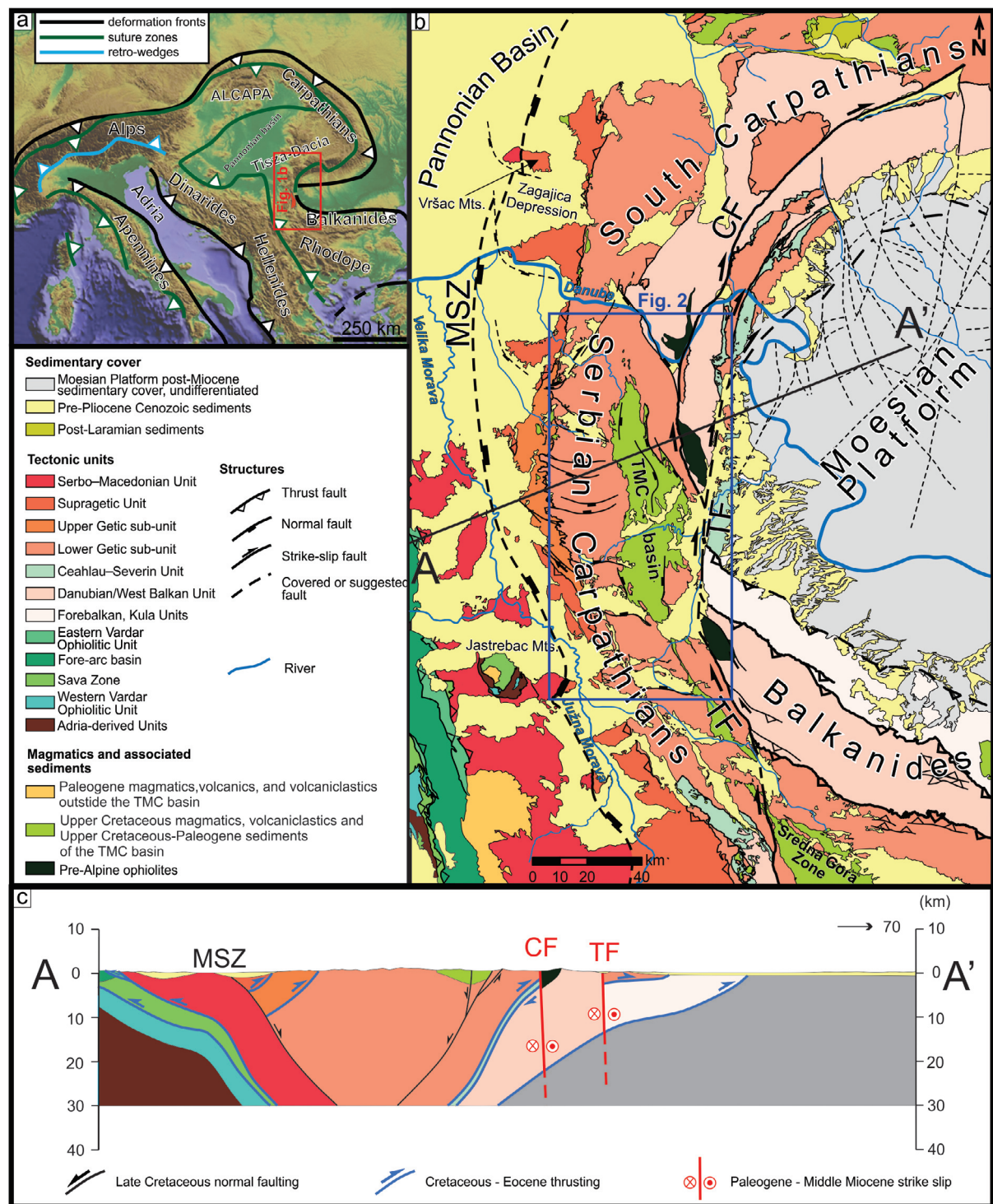


**Fig. 1. a)** Topographic map of Central Mediterranean orogens, displaying suture zones, orogenic fronts, and retro-wedges (modified after KRSTEKANIĆ et al., 2020). The red polygon represents the Late Cretaceous basin hosting the Timok Magmatic Complex (TMC), while the red rectangle indicates the location of the tectonic map in Figure 1b: **b)** Regional tectonic map of the area connecting the Dinarides and South Carpathians showing the main tectonic units of the Serbian Carpathians (modified after Schmid et al., 2008, 2020). The black line indicates the position of the A–A' cross-section shown in Fig. 1c, while the blue rectangle indicates the location of the geological map in Figure 2: **c)** Regional cross-section across the Serbian Carpathians and their transition to the Dinarides, twice vertically exaggerated. The main fault ages are shown in the legend, while colours of tectonic units correspond to those from Fig. 1b. **CF** – Cerna Fault; **TF** – Timok Fault; **MSZ** – Morava Shear Zone.



bolite-facies metamorphic basement, unconformably overlain by Late Carboniferous to Mesozoic sedimentary cover (PETKOVIĆ, 1975; KALENIĆ et al., 1980; DJORDJEVIĆ-MILUTINOVIĆ, 2010). The Mesozoic succession is generally composed of Middle Triassic to Lower Cretaceous carbonate platform deposits. These units were structured primarily as a result of the Mid-Cretaceous top-E thrusting event, induced by the initial closure of the Ceahlău-Severin Ocean (KRSTEKANIĆ et al., 2020). The subsequent Late Cretaceous extension resulted in the formation of the TMC Basin over the Getic Unit, accompanied by coeval calc-alkaline magmatism (VON QUADT et al., 2005; GALLHOFER et al., 2015). This is commonly interpreted as back-arc processes induced by steepening and retreating of the Neotethyan slab (VON QUADT et al., 2005; SCHMID et al., 2008; KOLB et al., 2013). Moreover, the TMC Basin is unconformably overlain by Paleogene sedimentary cover, exposed in the southern parts of the basin (Fig. 2 and Supplementary Fig. 1).

The more external Ceahlău-Severin Unit represents the remnants of a narrow oceanic rift that opened between the Dacia and European continent during the Early to Middle Jurassic (SCHMID et al., 2008, 2020). The basement of this unit is composed of ophiolitic lithologies, including ultramafics, gabbros, and pillow basalts, while the overlying sedimentary deposits include Late Jurassic radiolarites followed by Early Cretaceous terrigenous turbidites. The Danubian nappe sequence represents the original parts of the Moesian Platform that were included in the Carpathian nappe stack by the latest Cretaceous – earliest Paleogene eastward thrusting that accommodated the final closure of the Ceahlău-Severin Ocean (SÂNDULESCU, 1988; CSONTOS & VÖRÖS, 2004; IANCU et al., 2005; SEGHEDEI et al., 2005; NEUBAUER, 2015). The Danubian Unit consists of the Neoproterozoic basement, Paleozoic succession deformed and metamorphosed during the Variscan orogeny, and the Carboniferous to Late Cretaceous sedimentary cover. Following Late Cretaceous – Paleogene nappe emplacement, the basement of the Danubian Unit was exhumed at the surface during the Late Eocene – Oligocene as a result of orogen-parallel extension (FÜGENSCHUH & SCHMID, 2005).

## Late Oligocene – Middle Miocene oroclinal bending

After the final closure of the Ceahlău-Severin Ocean and subsequent collision, the Serbian Carpathians nappe stack was affected by subsequent Late Oligocene – Middle Miocene deformation driven by the indentation around the Moesian promontory and partially coeval roll-back subduction of the Carpathian slab in the Eastern Carpathians (SÂNDULESCU, 1988; CSONTOS & VÖRÖS, 2004; USTASZEWSKI et al., 2008; MATENCO & RADIVOJEVIĆ, 2012). Such along-strike changes in collisional mechanics resulted in the present-day orogenic curvature accompanied by the large-scale translations and rotations around the vertical axis (MÁRTON et al., 2024; VAN HINSBERGEN et al., 2008). At the crustal-scale, this resulted in significant strain partitioning characterized by the simultaneous formation of various structures with distinct kinematics that together form the Circum-Moesian Fault System (KRSTEKANIĆ et al., 2021, 2022).

The most dominant structures observed within this fault system in the Serbian part of the Carpathians are large-scale dextral strike-slip faults (Figs. 1b and 2). The initial deformation was accommodated by the formation of the Cerna Fault in the northern parts of the orogen (BERZA & DRĂGĂNESCU, 1988; KRÄUTNER & KRSTIĆ, 2002). As deformation progressed and Carpathian slab roll-back initiated around 20 Ma (MATENCO & RADIVOJEVIĆ, 2012), the late-stage structural pattern accommodating translations and rotations became more complex, which included the formation of several large-scale dextral faults that generally follow the orogenic trend (Fig. 2). These are N–S oriented Timok Fault and NW–SE oriented Sokobanja-Zvonce (SZF) and Rtanj-Pirot (RPF) dextral faults, previously defined by KRSTEKANIĆ et al. (2022). In its northern and central parts, the Timok Fault is defined by numerous lower-offset normal, oblique, and strike-slip faults that together form the negative flower structure and cross-cut the Cerna Fault (Fig. 2), accommodating the opening of the Donji Milanovac, Timok, and Knjaževac Middle Miocene intra-montane pull-apart basins (KRSTEKANIĆ et al., 2022; Fig. 2). West of the Timok Faults, the Sumrakovac, Šarbanovac, and Slatina Miocene basins unconformably overlie the



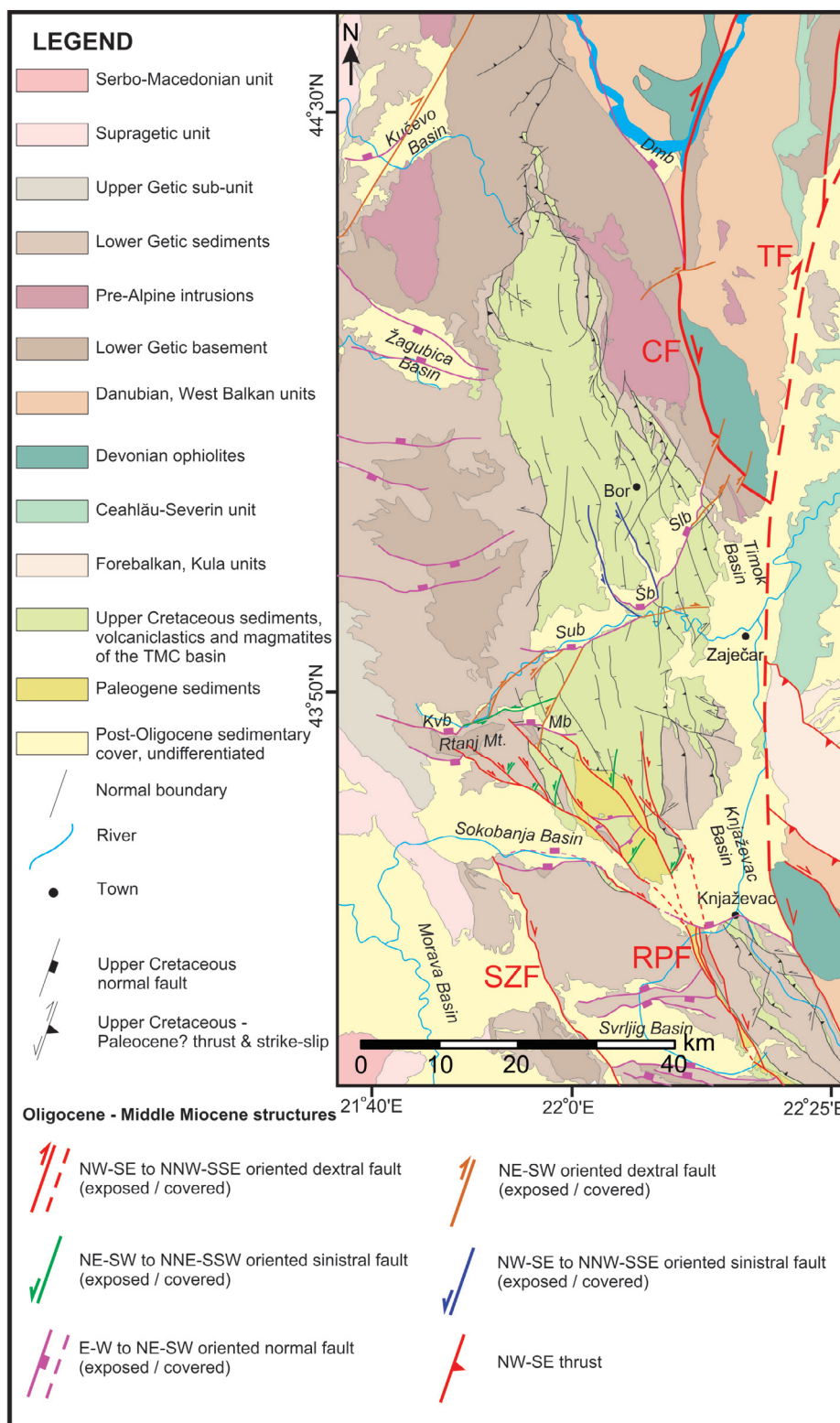


**Fig. 2.** Geological map of the Serbian Carpathians and adjacent areas of the South Carpathians and Balkanides showing the Oligocene – Middle Miocene structures (modified after KRSTEKANIĆ et al., 2020, 2022). The map is compiled from 1:100.000 maps of former Yugoslavia, modified with the results of previous (KRSTEKANIĆ et al., 2020; 2022) and this study. Faults covered with Neogene sediments are marked as dashed lines. **CF** – Cerna Fault; **TF** – Timok Fault; **SZF** – Sokobanja-Zvonce Fault; **RPF** – Rtanj-Pirot Fault; **Dmb** – Donji Milanovac Basin, **Slb** – Slatina Basin, **Šb** – Šarbanovac Basin, **Sub** – Sumrakovac Basin, **Kvb** – Krivi Vir Basin, **Mb** – Mirovo Basin.

Late Cretaceous volcano-sedimentary succession of the TMC basin (Fig. 2). These basins are interconnected and form a system of generally NE-SW elongated basins. Along the contact between these adjacent basins, narrow km-scale NNW-SSE oriented corridors of Miocene sediments are exposed as well. Southwards, strike-slip deformation along the Timok Fault is gradually transferred into the thrusting of the Balkanides (KRSTEKANIĆ et al., 2022).

The southern parts of the Circum-Moesian Fault System are marked by the Sokobanja-Zvonce and Rtanj-Pirot faults that are parallel to each other (Fig. 2) but show distinct kinematics. The first display a geometry resulted from a transtensional regime and, together with associated orogen-perpendicular normal faults, controlled the opening of several Middle Miocene intra-montane basins, such as the Sokobanja and Svrlijig basins (Fig. 2). In contrast, the Rtanj-Pirot Fault predominantly exhibits transpressive related deformation with locally developed transtensive character in the area of the Rtanj Mt., where the fault splays into multiple branches forming a horse-tail structure (KRSTEKANIĆ et al., 2022).

## Methodology

A detailed field structural and kinematic study was conducted within the Timok Magmatic Complex (TMC) basin and along its margins in the Serbian Carpathians. The main goal of this study was to determine and characterize the kinematics of the structures that post-date Late Cretaceous extension and latest Cretaceous – earliest Paleogene basin inversion (VESELINOVIĆ et al., 1970, 1975; Kalenić et al., 1976), by in field observation and structural analysis. The initial stage of analysis included re-interpretation of faults and fault zones using the 1:100 000 scale Basic Geological Maps of the former Yugoslavia and recent publications (DIMITRIJEVIĆ, 1997; MAROVIĆ et al., 2007; KRSTEKANIĆ et al., 2020, 2022). These maps were used to identify the geological features such as Miocene basins or exhumed basement zones and to establish correlations with neighbouring areas in the Serbian Carpathians. In order to constrain the relative timing of deformation, we con-

sider stratigraphic offsets along the map-scale faults and post-kinematic sedimentary cover.

Our fieldwork was focused on measuring the brittle structures along major faults and fault zones by using the kinematic indicators and superposition criteria. Observations also included cross-cutting relationships and block tilting or rotation. Collected measurements involved faults, fault gouges, shear zones, and folds. Kinematic indicators such as slickensides, striations, slickenfibres, Riedel shears, or syn-kinematic growth of secondary minerals, with considered confidence level and observation quality, were used to determine the fault type and displacement direction. Fold analysis focused on their geometry and the orientation of axial planes and fold axes. Structures that exhibit mutual cross-cutting overprint are considered within a single deformation event. In total, 173 structural measurements of six distinct structural types were collected (see Supplementary Table 1.).

Previous studies have shown that the Serbian Carpathians were affected by large-scale rotations and translations that caused significant strain partitioning at the crustal-scale (VAN HINSBERGEN et al., 2020; KRSTEKANIĆ et al., 2021, 2022; MÁRTON et al., 2024). In more detail, the study area accommodated coeval extension, shortening, and strike-slip deformation, which formed a complex system of connected structures with different type, kinematics, and orientation, typical for strike-slip related tectonics. Therefore, the collected dataset cannot be used for determining the paleostress directions, as it does not fulfil the Wallace-Bott criteria and other limitations defined by previous studies (e.g., SIMÓN, 2019; SPERNER & ZWIGEL, 2010).

The structural data were classified based on their location, type, orientation, and cross-cutting relationships and plotted in the Win-Tensor software (DELVAUX & SPERNER, 2003). This method allowed us to separate three distinct deformation phases. However, the present study is focused only on the latest deformation. The first two phases are not discussed in detail and are shown only to demonstrate cross-cutting relationships and confirm the relative timing of the youngest deformation event. Field observations and interpretations related to the Upper Cretaceous – Paleocene deformation are beyond the scope of this study.

## Results

### Southern part of the study area

In the southern part of the study area, a system of closely spaced NW-SE Ft1 dextral faults is observed in Paleogene limestones south of the Middle Miocene Knjaževac Basin (Ft1 in point 1, Fig. 3a; Fig. 4a). These structures exhibit transpressive deformation, as evidenced by striations and associated pervasive system of small-scale opened f1 folds with sub-horizontal axial planes and hinges parallel to the fault strike (f1 in point 1, Fig. 3a; Fig. 4a).

From point 1 northward and northwestward, F1 strike-slip faults exhibit a minor normal component. Along the southeastern margin of the TMC basin, these structures have dominant NNW-SSE orientations (Ft1 in point 2, Ft1 in points 5 & 6, Fig. 3a), while on the southeastern slopes of the Rtanj Mt. they trend WNW-ESE and locally display oblique-slip kinematics (Ft1 in points 4, 8 & 9, Fig. 3a). These faults cut through Lower Cretaceous limestones, overlying Upper Cretaceous volcano-clastic succession or Paleogene strata, and occur as isolated structures or closely spaced fault systems with well-defined striations, Riedel shears, and sporadic cm to m-scale brecciated fault zones (Fig. 4b). In some outcrops, these structures appear as negative flower structures associated with NW-SE oriented oblique normal faults or E-W trending Fn1 normal faults that indicate N-S to NNW-SSE direction of extension (Fn1 in point 2, Fig. 3a; Fig. 4c). The latter is also observed as individual fault planes in Devonian metasandstones along the northern margin of the Middle Miocene Sokobanja Basin (Fn1 in point 8, Fig. 3a) and Jurassic limestones along the southern margin of the Miocene Mirovo Basin (Fn1 in point 10, Fig. 3a). Furthermore, Ft1 dextral strike-slip faults are on the outcrops frequently associated with a NE-SW oriented conjugate set of Ft2 sinistral strike-slip faults, which also exhibit transtensional kinematics (Ft2 in point 3, Ft2 in point 7, Ft2 in points 8 & 9, Ft2 in point 10, Fig. 3a). The kinematics of Ft1 and Ft2 strike-slip and Fn1 normal faults is mostly determined by well-developed striations and calcite slickenfibres on fault planes. Furthermore, these structures quite often display mutual

cross-cutting relationships. For instance, at point 9 (Fig. 3map), WNW-ESE oriented Ft1 faults truncate NE-SW oriented conjugate Ft2 sinistral and NE-SW to E-W trending Fn1 normal faults (Fig. 4d). In other cases, (e.g., Point 8, on Fig. 3 map), Ft2 sinistral faults truncate or reactivate Fn1 normal faults on the same fault plane (Fig. 4e).

### Central and northern parts of the study area

In the central parts of the study area, Fn1 normal faults are the most observed type of structure. They are well-exposed in Late Cretaceous magmatics, volcanoclastics, and associated sediments situated along the northwestern and southeastern margins of the Miocene Sumrakovac, Šarbanovac, and Slatina basins (Fig. 3map). In contrast, Fn1 faults are not observed within the Miocene sediments. These structures are generally NE-SW to ENE-WSW oriented, with locally developed fault gouges and kinematic indicators such as striations, grooves, or Riedel shears (Figs. 5 a,b) that indicate NW-SE oriented extension (Fn1 in points 12 & 13, Fn1 in point 14, Fn1 in points 16, 17 & 18, Fig. 3b). On the outcrop scale, Fn1 normal faults exhibit clear cross-cutting relationships with the pre-existing structures. For instance, on the southern margin of the Slatina Basin, these structures cross-cut or reactivate the pre-existing NNE-SSW oriented transpressive dextral faults and meter-scale N-S oriented andesite dykes (points 13 & 14, on Fig. 3 map; e.g., Fig. 5c). Moreover, Fn1 normal faults are often exposed together with another set of NNW-SSE oriented Ft4 sinistral faults on the outcrops (Ft4 in points 13 & 16, Ft4 in points 17 & 18, Fig. 3b), where they cross-cut each other (Fig. 5c). On the southeastern margin of the Miocene Slatina Basin, Fn1 normal faults are in Late Cretaceous andesites and associated volcanoclastic rocks gradually replaced by oblique- to strike-slip Ft3 dextral faults that in some outcrops reactivate the pre-existing tension gashes filled up with secondary minerals (Ft3 in point 15, Fig. 3b). Ft3 dextral faults are also observed south of the Slatina and Šarbanovac basins in Lower Cretaceous limestones, where they exhibit more E-W orientation of the fault planes (Ft3 in point 11, Fig. 3b).



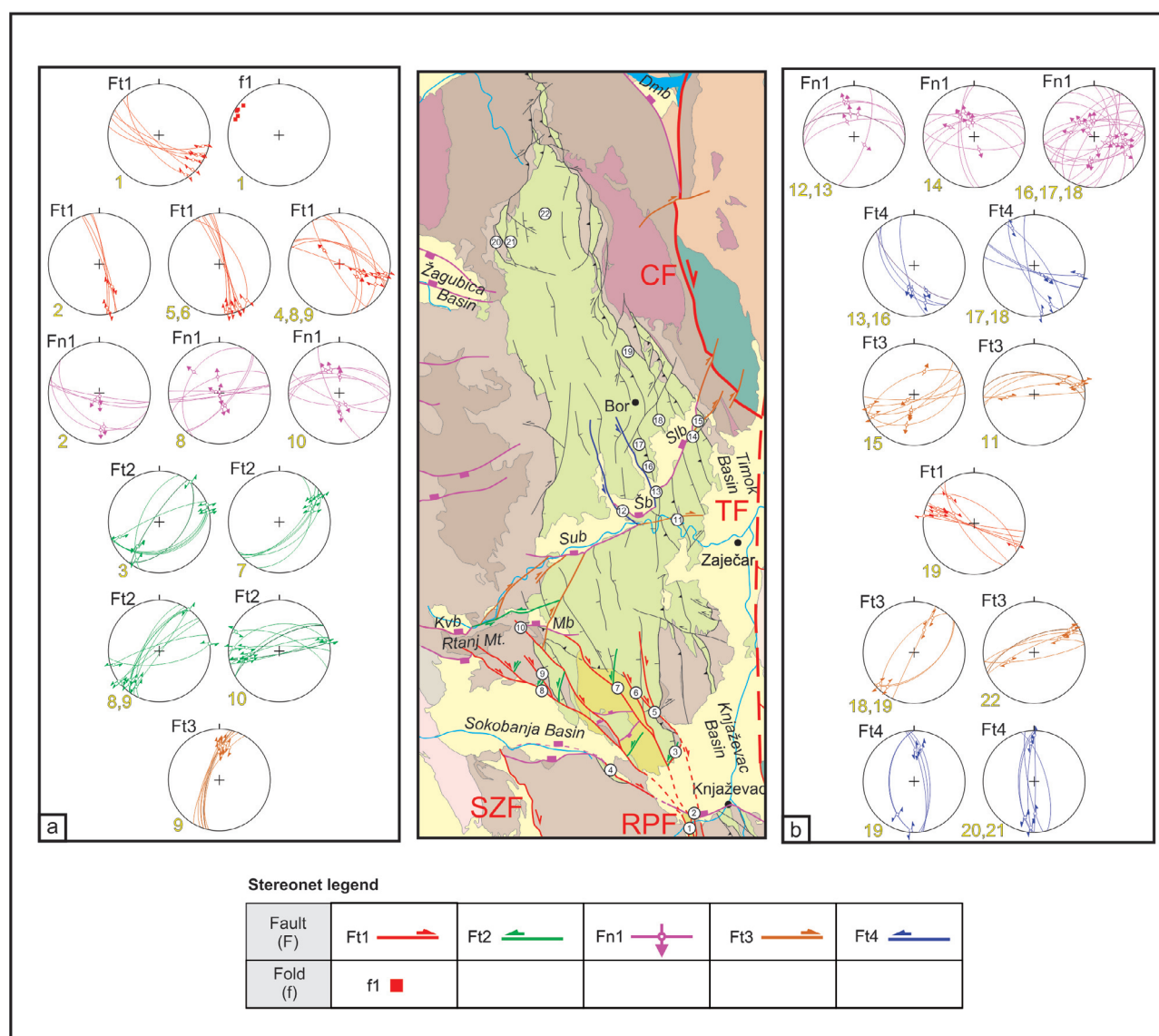


**Fig. 3.** Lower hemisphere stereoplots of the observed Oligocene – Middle Miocene structures with their location in the geological map of the studied area. Numbers in white circles represent the studied point on the map. Observed outcrop-scale structures of the study area were grouped into two fields, marking the kinematics of two different parts of the study area. The left rectangle represents structures in the southern parts of the study area (a), while the right rectangle displays structures from the central and northern parts of the study area (b). Each stereonet is marked with a structure type in the upper left corner (black colour), and the number of the observation point on the map (yellow colour). Stereonet legend: **f1** – fold with NW–SE oriented hinge and subhorizontal axial plane, **Ft1** – NW–SE to NNW–SSE oriented dextral fault, **Ft2** – NE–SW to NNE–SSW oriented sinistral fault, **Fn1** – E–W to NE–SW oriented normal fault, **Ft3** – NE–SW oriented dextral fault, **Ft4** – NW–SE to NNW–SSE oriented sinistral fault.

In the northern and northeastern parts of the TMC Basin, three distinct groups of strike-slip faults can be recognized. The first set of structures are NW–SE to WNW–ESE oriented Ft1 dextral faults (Ft1 in point 19, Fig. 3b). These faults are well-developed in Late Cretaceous andesites on the northeastern margin of the TMC Basin, where they are exposed as a system of closely spaced sub-vertical

fault planes with developed striations and slicken-fibres that indicate transtensional kinematics. On the outcrops, Ft1 dextral faults often truncate the pre-existing NE–SW oriented transpressive dextral faults (Fig. 5d). The other two sets of strike-slip faults represent a conjugate set of NE–SW oriented Ft3 dextral (Ft3 in points 18 & 19, Ft3 in point 22, Fig. 3b) and NNW–SSE to N–S trending Ft4 sinis-

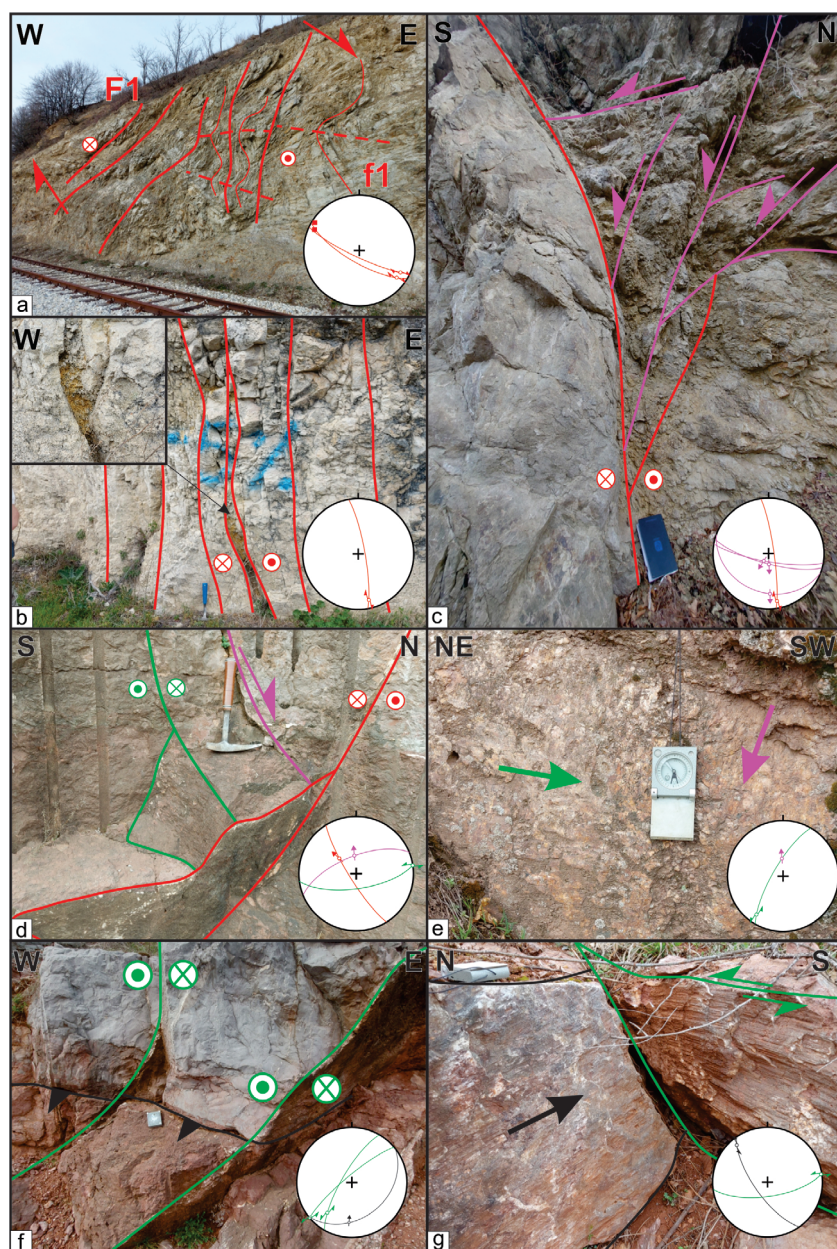


**Fig. 4.** Interpreted field photos of structures belonging to the Rtanj–Piroć Fault system in the southern parts of the study area. The orientation of each photo is indicated in the upper right and upper left corners. Structures are plotted on the stereoplots of each photo in the lower right corner. The locations of photos are displayed in the points of the Fig. 3map. Thicker red lines demonstrate Ft1 fault planes, while thinner red lines mark limbs of associated f1 folds. Dashed red lines represent axial planes of f1 folds. Purple lines and arrows indicate Fn1 normal faults, while red lines and arrows mark Ft2 sinistral faults. Note that pre-existing Late Cretaceous – Paleogene structures are marked by black lines and arrows. **a)** System of NW–SE oriented transpressive Ft1 strike-slip faults in Paleogene sediments accompanied by meter-scale f1 folds with hinges parallel to Ft1 fault planes. Point 1 ( $43^{\circ}32'44.86''\text{N } 22^{\circ}11'14.18''\text{E}$ ). **b)** Sub-vertical pervasive Ft1 dextral faults in Lower Cretaceous massive limestones. The inset displays cm-scale fault breccia. Point 5 ( $43^{\circ}40'42.35''\text{N } 22^{\circ}7'46.78''\text{E}$ ). **c)** Negative flower structure in Late Cretaceous volcanoclastics marked by sub-vertical NNW–SSE oriented Ft1 dextral and associated Fn1 normal fault with top-S kinematics. Point 2 ( $43^{\circ}32'41.28''\text{N } 22^{\circ}11'51.71''\text{E}$ ). **d)** Meter-scale NW–SE oriented Ft1 dextral fault truncating ENE–WSW oriented Ft2 sinistral and ENE–WSW oriented Fn1 normal faults in Lower Cretaceous limestones. Point 9 ( $43^{\circ}43'49.77''\text{N } 21^{\circ}57'10.77''\text{E}$ ). **e)** NE–SW oriented Ft2 sinistral fault in Late Cretaceous conglomerates reactivating Fn1 normal fault on the same fault plane. Point 8 ( $43^{\circ}43'8.77''\text{N } 21^{\circ}56'45.30''\text{E}$ ). **f)** NE–SW oriented sinistral strike-slip fault cross-cutting pre-Eocene low-angle thrust with top-NNE direction of tectonic transport. Point 9 ( $43^{\circ}43'49.77''\text{N } 21^{\circ}57'10.77''\text{E}$ ). **g)** Meter-scale pre-Eocene sinistral fault with NW–SE oriented fault plane and reverse component truncated by ENE–WSW trending Ft2 sinistral strike-slip. Point 9 ( $43^{\circ}43'49.77''\text{N } 21^{\circ}57'10.77''\text{E}$ ).



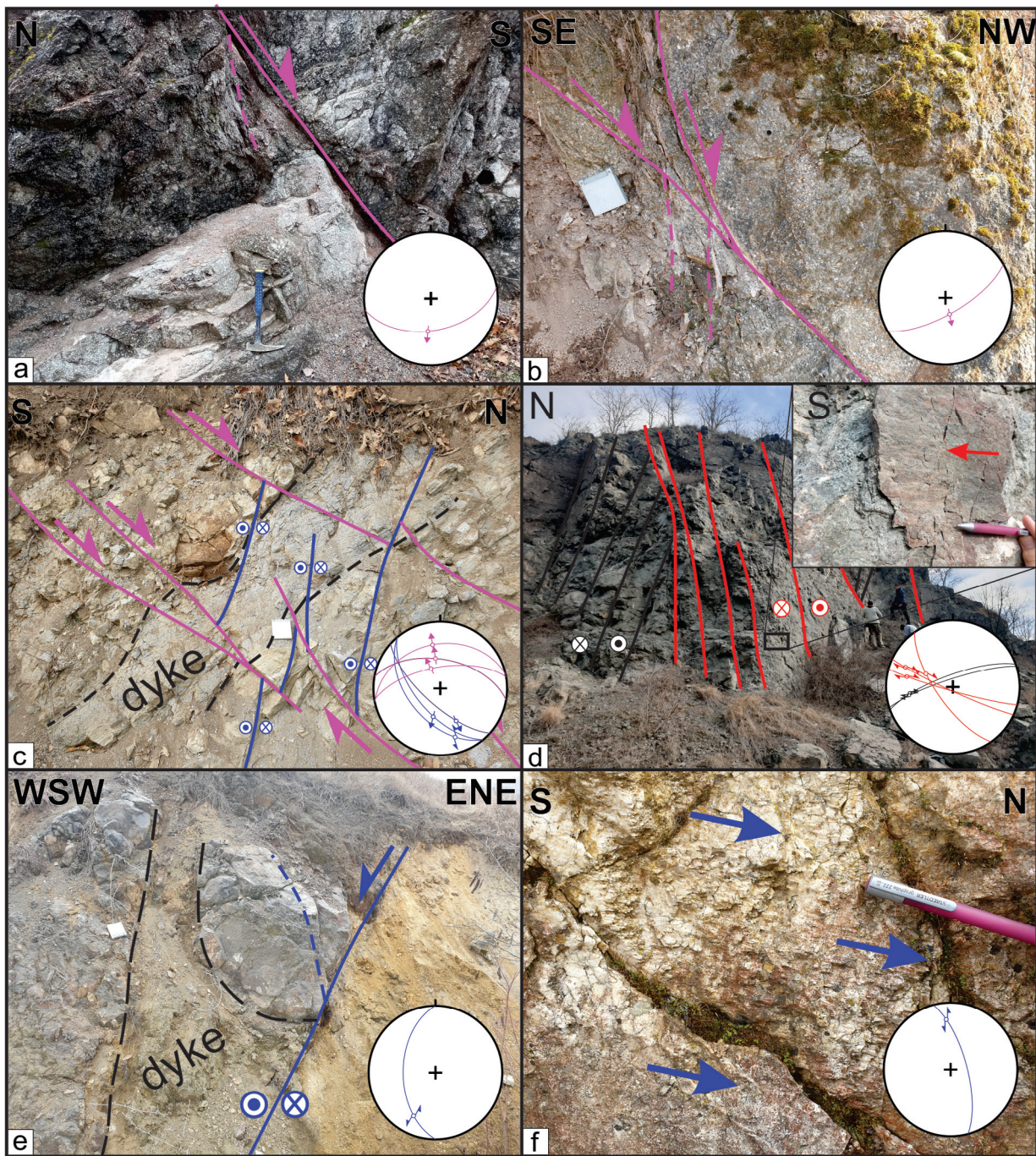


**Fig. 5.** Interpreted field photos of Oligocene – Middle Miocene extensional and strike-slip structures in the central and northern parts of the study area. The orientation of each photo is indicated in the upper right and upper left corners. Structures are plotted on the stereoplots of each photo in the lower right corner. The locations of photos are displayed in the points of the Fig. 3map. Purple lines and arrows indicate Fn1 normal faults, while dashed purple lines mark associated Riedel shears. The blue lines and arrows represent Ft4 sinistral strike-slip faults. Dashed black lines indicate contact between dyke intrusions and host rocks, while black lines demonstrate pre-Eocene transpressive structures. **a-b)** ENE-WSW oriented Fn1 normal faults with associated Riedel shears in Late Cretaceous andesites. Point 17 ( $44^{\circ}1'33.00''N$   $22^{\circ}6'17.00''E$ ). **c)** Meters-scale andesite dyke cross-cut by Fn1 normal faults with top-N kinematics and NW-SE oriented Ft4 sinistral faults. Note the mutual cross-cutting relationships between Fn1 and Ft4. Point 13 ( $43^{\circ}57'46.00''N$   $22^{\circ}8'9.00''E$ ). **d)** Closely spaced system of ESE-WNW oriented transpressive dextral Ft1 faults with slickenfibres truncating pre-Eocene ENE-WSW trending transpressive dextral fault in Late Cretaceous andesites. Point 19 ( $44^{\circ}7'57.09''N$   $22^{\circ}5'25.88''E$ ). **e)** Meter-scale dyke and associated volcanoclastics cross-cut by N-S oriented Ft4 strike-slip fault. Point 19 ( $44^{\circ}7'56.03''N$   $22^{\circ}6'7.99''E$ ). **f)** NNW-SSE oriented Ft4 sinistral fault with well-developed grooves in Late Jurassic massive limestones. Point 20 ( $44^{\circ}16'46.03''N$   $21^{\circ}51'45.29''E$ ).



tral transtensional faults (Ft4 in point 19, Ft4 in points 20 & 21, Fig. 3b). Both Ft3 and Ft4 faults on the outcrops made up by Late Cretaceous volcano-sedimentary succession exhibit clear superposition with the pre-existing structures. At point 19, NE–SW oriented Ft3 dextral faults are locally observed to reactivate dextral transpressive faults along the same fault planes. In other cases, the conjugate Ft4 sinistral faults truncate meter-scale NW–SE trending magmatic andesite dykes (Fig. 5e). In addition, Ft4 faults are also documented in Upper Jurassic massive limestones on the northwestern margin of the TMC basin, where they display sinistral kinematics by well-developed grooves (Fig. 5f). Although the cross-cutting relationships between these three sets of strike-slip faults and older structures are well constrained, mutual cross-cutting interplay between Ft1 and conjugate Ft3–Ft4 faults has not been observed in the field.

## Interpretation

### Connecting the observed structures with the Circum-Moesian fault system

Field kinematics and superposition relations indicate that the most prominent Ft1 dextral faults in the southern parts of the TMC Basin and underlying Getic Unit represent a generally NW–SE oriented map-scale structure that aligns in kinematics, geometry, and timing with the previously defined Late Oligocene – Middle Miocene Rtanj-Pirot Fault (KRSTEKANIĆ et al., 2022; RPF in Fig. 2). In the southernmost parts of the study area, the Rtanj-Pirot Fault is marked by a narrow and transpressive fault zone that affects the Upper Cretaceous volcano-sedimentary succession and overlying Paleogene sediments. Northward and northwestward, the Rtanj-Pirot Fault splays into lower-offset NW- and NNW-striking segments, forming a transtensional horse-tail structure. These splays are linked to conjugate Ft2 sinistral and Fn1 normal faults, as evidenced by their mutual interplay in outcrops. Beyond the previously identified structural control of the Knjaževac, Sokobanja, and Krivi Vir basins (KRSTEKANIĆ et al., 2022; Figs. 2 and 3), our dataset indicates that

Fn1 normal faults accommodating N–S to NNW–SSE oriented extension likely controlled the formation of another, relatively small Mirovo Basin (Mb in Fig. 2). Moreover, normal faulting presumably contributed to the exhumation of Devonian metasediments exposed on the margin of several Miocene basins (Fig. 2).

From the northwestern periphery of the Rtanj-Pirot fault system towards the central parts of the TMC Basin, deformation appears to be partitioned by coeval strike-slip and extensional deformation, as inferred by conjugate Ft3–Ft4 and Fn1 normal faults. Although Ft3–Ft4 faults do not show clear cross-cutting relationships with Ft1–Ft2 strike-slip faults, both groups overprint Late Cretaceous magmatic intrusions or Latest Cretaceous–Paleogene transpressive structures on the outcrops. Furthermore, mutual cross-cutting relationships between Ft1 – Ft4 strike-slip faults and Fn1 normal faults indicate that they were formed during a single deformation phase.

The kinematics of Fn1 normal faults around the Slatina, Šarbanovac, and Sumrakovac Miocene basins, together with their NE–SW elongation, suggests that these basins were structurally controlled by normal faulting. The overall basin geometry, SEward thickening of Miocene sediments (e.g., the Slatina basin), topographic expression of pre-Miocene units, and generally NW-dip of Fn1 faults along the southeastern margin of the Slatina and Šarbanovac basins demonstrate that Fn1 normal faults on the southeastern margin accommodated the largest displacements. Such observations suggest that these Miocene basins are asymmetric with half-graben geometry. In more detail, the NW- to NNW-dipping normal faults along the southeastern margins appear to be the main structures accommodating the extension, while lower offset faults on the northwestern margins represent a system of synthetic and antithetic structures, likely connected with the main fault at depth. In addition, our data demonstrate that each basin is laterally segmented by NW–SE to NNW–SSE oriented Ft4 sinistral faults. We interpret these faults as small-scale transfer zones between individual half-grabens, potentially accommodating differential subsidence within the basins. From the Slatina basin north-

eastwards, NW–SE oriented extension is gradually transferred to strike-slip deformation, as inferred by the gradual change of Fn1 faults into oblique- or strike-slip Ft3 dextral faults (point 14, Fig. 3map).

Furthermore, Ft3 dextral faults extend beyond the TMC basin northeastwards, where they cross-cut and offset the regional Cerna Fault up to 2 km (Fig. 2).

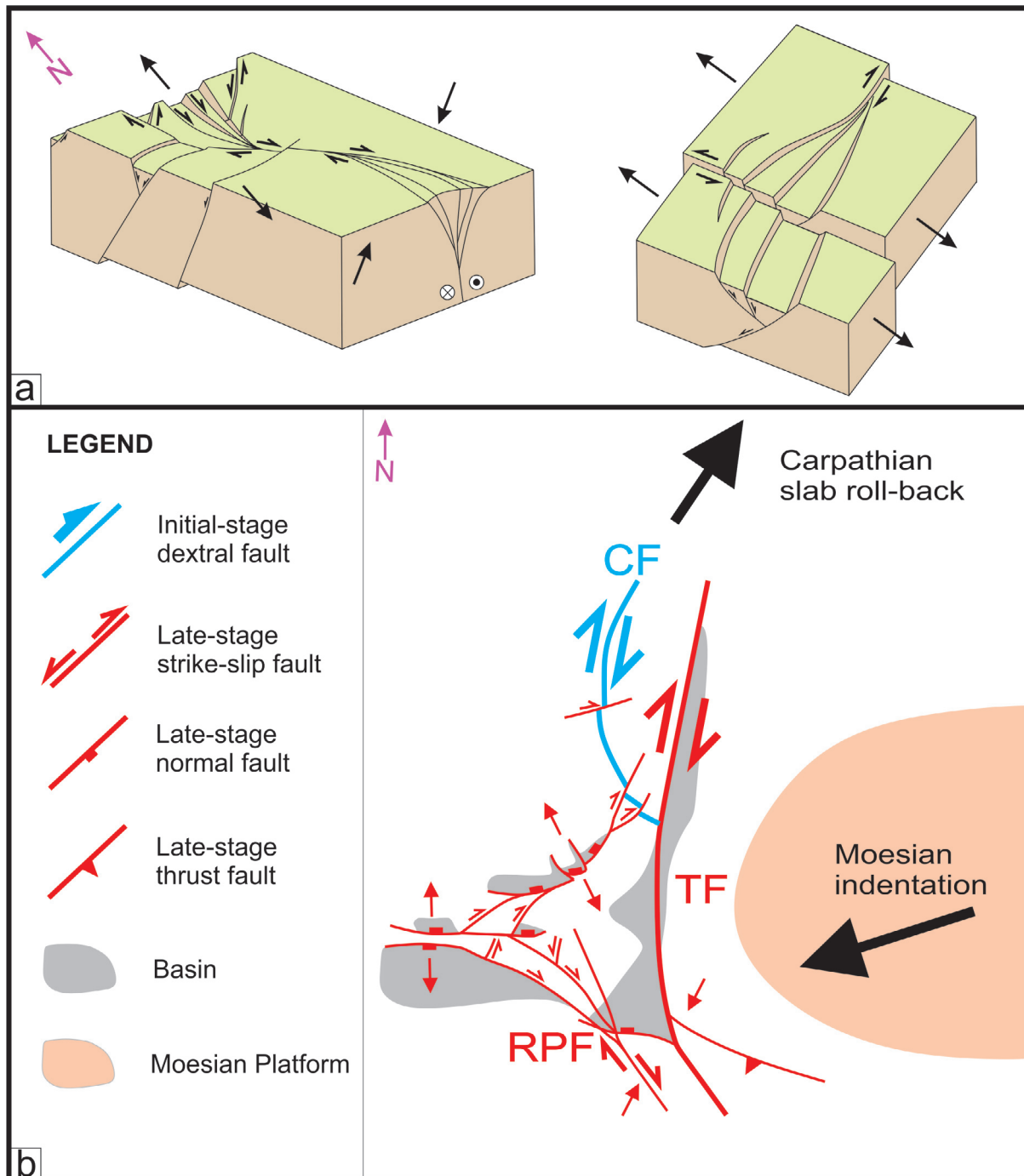


**Fig. 6.** Idealized 3D and map-view sketches of Oligocene – Middle Miocene deformation affecting the TMC basin and underlying Getic Unit. **a)** 3D block-diagram showing the mechanisms of strain partitioning along the Rtanj-Pirot Fault (left) and the opening of Slatina–Šarbanovac–Sumrakovac Miocene basins (right). The purple arrow in the upper left corner indicates the orientation of block diagrams. **b)** Simplified map-view of the main structures and associated basins affecting and overlying the TMC basin. Black arrows represent the main tectonic forces that induced strain partitioning.

In the northern parts of the study area, strike-slip deformation marked by Ft1 dextral and conjugate Ft3-Ft4 faults does not correspond well with the kinematics of map-scale structures within the TMC basin. However, recent studies suggest that these structures could be responsible for the rotation of the Late Cretaceous – earliest Paleogene dextral transpressive faults. A possible interpretation for Ft1 dextral faults along the northeastern margins of the TMC basin could be a local effect of large-scale dextral displacements associated with the Cerna Fault activity, as they exhibit almost the same orientation in this part of the Serbian Carpathians.

## Discussion

Our dataset demonstrates that observed structures within the TMC Basin and along its margins are part of the broader Circum-Moesian Fault System that accommodated indentation processes around the Moesian Platform (KRSTEKANIĆ et al., 2022). Structural patterns indicate that deformation was characterized by significant strain partitioning between extensional and transtensive structures that were further southeastward transferred into transpressive deformation (Fig. 6). Such a mechanism of strain partitioning is well correlative with the previous studies (KRSTEKANIĆ et al., 2021, 2022). The superposition criteria imply that the age of observed deformation post-dates Paleogene sedimentation and pre-dates the end of Middle Miocene deposition. Although the exact age of the Paleogene succession remains unconstrained, previous studies have demonstrated that dextral faults south of the study area deform Eocene sediments of the Babušnica basin as well (KRSTEKANIĆ et al., 2022). This implies that the onset of indentation related structures may have occurred slightly earlier than the previously proposed Late Oligocene. However, most of the observed structures within the TMC basin likely represent the late-stage structures of the Circum-Moesian Fault System, while only minor Ft1 faults developed along the northeastern margin of the TMC basin may be attributed to the early-stage deformation related to the Cerna Fault activity.

## Conclusions

Field structural and kinematic study from the Late Cretaceous basin hosting the Timok Magmatic Complex (TMC) demonstrates that this part of the Serbian Carpathians experienced significant strain partitioning during the Oligocene – Middle Miocene. The observed structures represent the parts of the broader Circum-Moesian Fault System, formed during Moesian indentation and accompanied Carpathian slab roll-back in the Eastern Carpathians. Our study builds upon and refines previously proposed models of crustal-scale deformation (KRSTEKANIĆ et al., 2021, 2022) by providing new structural data and kinematic analysis that confirm the progressive transition from extensional and transtensional strike-slip regimes along the orogenic strike into transpressive and contractional domains. Moreover, we indicate that intra-montane Miocene basins overlying the TMC basin were controlled by normal faulting.

## Acknowledgments

This research was supported by the Science Fund of the Republic of Serbia, Grant No. TF C1389-YF, Geodynamics of basins above subducted slabs: an integrated modelling study of tectonics, sedimentation, and magmatism in the Timok Magmatic Complex – TMCmod (Project No. 7461) and the Ministry of Education, Science, and Technological Development of the Republic of Serbia (Contract No. 451-03-136/2025-03/200126). We thank Editor NEVENKA ĐERIĆ, IOAN MUNTEANU and an anonymous reviewer for their constructive feedback, which significantly improved the quality of the original manuscript.

## References

- ANTIĆ, M., PEYTCHEVA I., VON QUADT, A., KOUNOV, A., TRIVIĆ, B., SERAFIMOVSKI, T., TASEV, G., GERDJKOV, I. & WETZEL, A., 2016. Pre-Alpine evolution of a segment of the North-Gondwanan margin: Geochronological and geochemical evidence from the central Serbo-Macedonian Massif. *Gondwana Research*, 36: 523–544.



- ANTIĆ, M.D., KOUNOV, A., TRIVIĆ, B., WETZEL, A., PEYTCEVA, I. & VON QUADT, A. 2016. Alpine thermal events in the central Serbo-Macedonian Massif (southeastern Serbia). *International Journal of Earth Sciences*, 105: 1485–1505.
- BERZA, T. & DRĂGĂNESCU, A. 1985. The Cerna–Jiu fault system (South Carpathians, Romania), a major Tertiary transcurrent lineament. *Dări de seamă ale şedinţelor. Institutul de Geologie şi Geofizică, Seria Geologie Tectonică şi Regională*, 72 (5): 43–57.
- DELVAUX, D. & SPERNER, B. 2003. New aspects of tectonic stress inversion with reference to the TENSOR program. *Geological Society, London, Special Publications*, 212 (1): 75–100.
- DIMITRIJEVIĆ, M.D. 1997. *Geology of Yugoslavia*. 2nd edition. Geoinstitute, Belgrade, 1–187.
- DJORDJEVIĆ-MILUTINOVIĆ, D. 2010. An overview of Paleozoic and Mesozoic sites with macroflora in Serbia. *Bulletin of the Natural History Museum*, 3: 27–46.
- FÜGENSCHUH, B. & SCHMID, S.M. 2005. Age and significance of core complex formation in a very curved orogen: Evidence from fission track studies in the South Carpathians (Romania). *Tectonophysics*, 404 (1–2): 33–53.
- GALLHOFFER, D., VON QUADT, A., PEYTCEVA, I., SCHMID, S.M. & HEINRICH, C.A. 2015. Tectonic, magmatic, and metallogenic evolution of the Late Cretaceous arc in the Carpathian–Balkan orogen. *Tectonics*, 34 (9): 1813–1836.
- HORVÁTH, F., MUSITZ, B., BALÁZS, A., VÉGH, A., UHRIN, A., NÁDOR, A., KOROKNAI, B., PAP, N., TÓTH, T. & WÓRUM, G. 2015. Evolution of the Pannonian Basin and its geothermal resources. *Geothermics*, 53: 328–352.
- IANCU, V., BERZA, T., SEGHEDI, A. & MARUNȚIU, M. 2005. Palaeozoic rock assemblages incorporated in the South Carpathian Alpine thrust belt (Romania and Serbia): a review. *Geologica Belgica*, 8 (4): 293–304.
- KALENIĆ, M., ĐORĐEVIĆ, M., KRSTIĆ, B., BOGDANOVIĆ, P., MILOŠAKOVIĆ, R., DIVLJAN, M., ČIČULIĆ, M., DŽODŽO, R., RUDOLF, L.J. & JOVANOVIĆ, L.J., 1976. Osnovna geološka karta SFRJ 1:100000. Tumač za list Bor L34-141 [*Basic Geologic Map of Former Yugoslavia 1:100 000. Explanatory booklet for the Sheet Bor* – in Serbian]. Savezni geološki zavod, Beograd.
- KALENIĆ, M., HADŽI-VUKOVIĆ, M., DOLIĆ, D., LONČAREVIĆ, Č. & RAKIĆ, O., 1980. Osnovna geološka karta SFRJ 1:100000. Tumač za list Kučevo L34-128 [*Basic Geologic Map of Former Yugoslavia 1:100 000. Explanatory booklet for the Sheet Kučevo* – in Serbian]. Savezni geološki zavod, Beograd.
- KOLB, M., VON QUADT, A., PEYTCEVA, I., HEINRICH, C.A., FOWLER, S.J. & CVETKOVIĆ, V. 2013. Adakite-like and normal arc magmas: distinct fractionation paths in the East Serbian segment of the Balkan–Carpathian arc. *Journal of Petrology*, 54 (3): 421–451.
- KRÄUTNER, H.G. & KRSTIĆ, B. 2002. Alpine and Pre-Alpine structural units within Southern Carpathians and the Eastern Balkanides. *Proceedings of XVII Congress of Carpathian-Balkan Geological Association, Bratislava, September 1–4. Geologica Carpathica*, 53, Special Issue.
- KRSTEKANIĆ, N., MATENCO, L., TOLJIĆ, M., MANDIĆ, O., STOJADINOVIC, U. & WILLINGSHOFER, E. 2020. Understanding partitioning of deformation in highly arcuate orogenic systems: Inferences from the evolution of the Serbian Carpathians. *Global and Planetary Change*, 195: 103361.
- KRSTEKANIĆ, N., WILLINGSHOFER, E., BROERSE, T., MATENCO, L., TOLJIĆ, M. & STOJADINOVIC, U. 2021. Analogue modelling of strain partitioning along a curved strike-slip fault system during backarc-convex orocline formation: Implications for the Cerna-Timok fault system of the Carpatho-Balkanides. *Journal of Structural Geology*, 149: 104386.
- KRSTEKANIĆ, N., MATENCO, L., STOJADINOVIC, U., WILLINGSHOFER, E., TOLJIĆ, M. & TAMMINGA, D. 2022. Strain partitioning in a large intracontinental strike-slip system accommodating backarc-convex orocline formation: The Circum-Moesian Fault System of the Carpatho-Balkanides. *Global and Planetary Change*, 208: 103714.
- MALEŠ, M., RANDELOVIĆ, N., KRSTEKANIĆ, N., KOSTIĆ, B., ČIRIĆ, N. & STOJADINOVIC, U. 2023. New insights into tectonic relations between the Eastern Vardar Ophiolitic and Serbo-Macedonian units: Inferences from a microtectonic study in central Serbia. *Geološki anali Balkanskeg poluostrva*, 84 (1): 33–45.
- MAROVIĆ, M., TOLJIĆ, M., RUNDIĆ, L. & MILIVOJEVIĆ, J., 2007. *Neoalpine Tectonics of Serbia*. Serbian Geological Society, Belgrade.
- MÁRTON, E., CVETKOV, V., BANJEŠEVIĆ, M., IMRE, G. & PAČEVSKI, A. 2024. Tectonic evolution of the Circum-Moesian orocline of the Carpatho-Balkanides: Paleomagnetic constraints. *Journal of Geodynamics*, 162: 102058.
- MATENCO, L. & RADIVOJEVIĆ, D. 2012. On the formation and evolution of the Pannonian Basin: Constraints derived from the structure of the junction area between the Carpathians and Dinarides. *Tectonics*, 31 (6): 1–20.

- MATENCO, L., MUNTEANU, I., TER BORGH, M., STĂNICĂ, A., TILITA, M., LERICOLAIS, G., DINU, C. & OAI, G. 2016. The interplay between tectonics, sediment dynamics and gateways evolution in the Danube system from the Pannonian Basin to the western Black Sea. *Science of the Total Environment*, 543: 807–827.
- MATENCO, L. 2017. Tectonics and exhumation of Romanian Carpathians: Inferences from kinematic and thermochronological studies. In: RĂDOANE, M. & VESPREMEANU-STROE, A. (Eds.). *Landform Dynamics and Evolution in Romania*. Springer Geography, Springer: 15–56.
- NEUBAUER, F. 2015. Cretaceous tectonics in Eastern Alps, Carpathians and Dinarides: Two-step microplate collision and Andean-type magmatic arc associated with orogenic collapse. *Rendiconti Online Società Geologica Italiana*, 37: 40–43.
- PAMIĆ, J. 2002. The Sava-Vardar Zone of the Dinarides and Hellenides versus the Vardar Ocean. *Eclogae Geologicae Helvetiae*, 95: 99–113.
- PETKOVIĆ, K. 1975. Geologija Srbije: Stratigrafija – Prekambrijum i Paleozoik [Geology of Serbia: Stratigraphy – Precambrian and Paleozoic]. In: Petković, K. (Ed.). *Geologija Srbije [Geology of Serbia]*. Faculty of Mining and Geology, Belgrade.
- RATSCHBACHER, L., LINZER, H.G., MOSER, F., STRUSIEVICZ, R.O., BEDELEAN, H., HAR, N. & MOĞOŞ, P.A. 1993. Cretaceous to Miocene thrusting and wrenching along the central South Carpathians due to a corner effect during collision and oroclinal formation. *Tectonics*, 12 (4): 855–873.
- SÂNDULESCU, M. 1988. Cenozoic tectonic history of the Carpathians. In: ROYDEN, L.H. & HORVÁTH, F. (Eds.). *The Pannonian Basin: A Study in Basin Evolution*. AAPG Memoir 45, American Association of Petroleum Geologists, Tulsa, OK: 17–25.
- SCHMID, S.M., BERNOULLI, D., FÜGENSCHUH, B., MATENCO, L., SCHEFER, S., SCHUSTER, R., TISCHLER, M. & USTASZEWSKI, K. 2008. The Alpine-Carpathian-Dinaridic orogenic system: Correlation and evolution of tectonic units. *Swiss Journal of Geosciences*, 101: 139–183.
- SCHMID, S.M., FÜGENSCHUH, B., KOUNOV, A., MATENCO, L., NIEVERGELT, P., OBERHÄNSLI, R., PLEUGER, J., SCHEFER, S., SCHUSTER, R., TOMLJENOVIC, B. & USTASZEWSKI, K. 2020. Tectonic units of the Alpine collision zone between Eastern Alps and western Turkey. *Gondwana Research*, 78: 308–374.
- SEGHEDEI, A., BERZA, T., IANCU, V., MARUNȚIU, M. & OAI, G. 2005. Neoproterozoic terranes in the Moesian basement and in the Alpine Danubian nappes of the South Carpathians. *Geologica Belgica*, 8: 4–19.
- SIMON, J.L. 2019. Forty years of paleostress analysis: Has it attained maturity? *Journal of Structural Geology*, 125: 124–133.
- SPERNER, B. & ZWIEGEL, P. 2010. A plea for more caution in fault-slip analysis. *Tectonophysics*, 482 (1–4): 29–41.
- STOJADINOVIC, U., KRSTEKANIC, N., KOSTIC, B., RUŽIĆ, M. & LUKOVIĆ, A. 2021. Tectonic evolution of the Vršac Mts. (NE Serbia): Inferences from field kinematic and microstructural investigations. *Geologica Carpathica*, 72 (5): 395–405.
- STOJADINOVIC, U., KRSTEKANIC, N., MATENCO, L. & BOGDANOVIĆ, T. 2022. Towards resolving Cretaceous to Miocene kinematics of the Adria–Europe contact zone in reconstructions: Inferences from a structural study in a critical Dinarides area. *Terra Nova*, 34 (6): 523–534.
- STOJADINOVIC, U., POMELLA, H., KRSTEKANIC, N., KOSTIC, B., MALEŠ, M., RANĐELOVIĆ, N. & RADONJIĆ, M. 2024. Exhumation history of the Juhor Mts. in Central Serbia, the Northern Serbo–Macedonian Subunit. *Geologica Carpathica*, 75 (3): 213–223.
- TOLJIĆ, M., MATENCO, L., STOJADINOVIC, U., WILLINGSHOFER, E. & LJUBOVIĆ-OBRAĐOVIĆ, D. 2018. Understanding fossil fore-arc basins: Inferences from the Cretaceous Adria–Europe convergence in the NE Dinarides. *Global and Planetary Change*, 171: 167–184.
- USTASZEWSKI, K., SCHMID, S.M., FÜGENSCHUH, B., TISCHLER, M., KISSLING, E. & SPAKMAN, W. 2008. A map-view restoration of the Alpine–Carpathian–Dinaridic system for the Early Miocene. *Swiss Journal of Geosciences*, 101: 273–294.
- USTASZEWSKI, K., SCHMID, S.M., LUGOVIĆ, B., SCHUSTER, R., SCHALTEGGER, U., BERNOULLI, D., HOTTINGER, L., KOUNOV, A., FÜGENSCHUH, B. & SCHEFER, S. 2009. Late Cretaceous intra-oceanic magmatism in the internal Dinarides (northern Bosnia and Herzegovina): Implications for the collision of the Adriatic and European plates. *Lithos*, 108: 106–125.
- VAN HINSBERGEN, D.J., DUPONT-NIVET, G., NAKOV, R., OUD, K. & PANAIOTU, C. 2008. No significant post-Eocene rotation of the Moesian Platform and Rhodope (Bulgaria): Implications for the kinematic evolution of the Carpathian and Aegean arcs. *Earth and Planetary Science Letters*, 273 (3–4): 345–358.
- VAN HINSBERGEN, D.J., TORSVIK, T.H., SCHMID, S.M., MATENCO, L.C., MAFFIONE, M., VISSERS, R.L., GÜRER, D. & SPAKMAN, W.

2020. Orogenic architecture of the Mediterranean region and kinematic reconstruction of its tectonic evolution since the Triassic. *Gondwana Research*, 81: 79–229.

VESELINović, M., ANTONIJEVIĆ, I., MILOŠAKOVIĆ, R., MIĆIĆ, I., KRSTIĆ, B., ČIČULIĆ, M., DIVLJAN, M. & MASLAREVIĆ, LJ. 1970. Osnovna geološka karta SFRJ 1:100 000. Tumač za list Boljevac K34-8 [*Basic Geologic Map of Former Yugoslavia 1:100 000. Explanatory booklet for the Sheet Boljevac* – in Serbian]. Savezni geološki zavod, Beograd.

VESELINović, M., DIVLJAN, M., ĐORĐEVIĆ, M., KALENIĆ, M., MILOŠAKOVIĆ, R., RAJČEVIĆ, D., POPOVIĆ, R. & RUDOLF, LJ. 1975. Osnovna geološka karta SFRJ 1:100 000. Tumač za list Zaječar K34-9 [*Basic Geologic Map of Former Yugoslavia 1:100 000. Explanatory booklet for the Sheet Zaječar* – in Serbian]. Savezni geološki zavod, Beograd.

VON QUADT, A.V., MORITZ, R., PEYTCHEVA, I. & HEINRICH, C.A. 2005. Geochronology and geodynamics of Late Cretaceous magmatism and Cu-Au mineralization in the Panagyurishte region of the Apuseni–Banat–Timok–Srednogorie belt, Bulgaria. *Ore Geology Reviews*, 27: 95–126.

## Резиме

### Деформација изазвана индентацијом у Српским Карпатима: Структурна и кинематска студија у басену Тимочког магматског комплекса и Доњој Гетској јединици

Структурна и кинематска теренска истраживања горњокредног басена који обухвата Тимочки магматски комплекс (ТМК) показују да је овај део српских Карпата претрпео значајну расподелу стреса током олигоцена и средњег миоцена. Опсервиране структуре представљају делове регионалног Циркум-Мезијског раседног система, који је формиран током индентације Мезије, уз истовремено повијање Карпатске плоче у источним Карпатима. Наша студија потврђује раније дефинисане механизме деформације у домену Земљине коре, где је извршен трансфер деформације дуж пружања орогена од екстензионих и транстензионих структура у транспресију и навлачење. Поред тога, наша студија први пут дефинише да су миоценски унутарпланински басени који леже трансгресивно преко ТМК басена били контролисани нормалним раседима.

*Manuscript received May 15, 2025*

*Revised manuscript accepted July 03, 2025*